


RESEARCH ARTICLE

Open Access



Analysis of genetically determined gene expression suggests role of inflammatory processes in exfoliation syndrome

Jibril B. Hirbo^{1,2*} , Francesca Pasutto³, Eric R. Gamazon^{1,2,4}, Patrick Evans¹, Priyanka Pawar⁵, Daniel Berner⁶, Julia Sealock¹, Ran Tao⁷, Peter S. Straub¹, Anuar I. Konkashbaev¹, Max A. Breyer¹, Ursula Schlötzer-Schrehardt⁶, André Reis³, Milam A. Brantley Jr⁴, Chiea C. Khor⁸, Karen M. Joos⁵ and Nancy J. Cox^{1,2}

Abstract

Background Exfoliation syndrome (XFS) is an age-related systemic disorder characterized by excessive production and progressive accumulation of abnormal extracellular material, with pathognomonic ocular manifestations. It is the most common cause of secondary glaucoma, resulting in widespread global blindness. The largest global meta-analysis of XFS in 123,457 multi-ethnic individuals from 24 countries identified seven loci with the strongest association signal in chr15q22–25 region near LOXL1. Expression analysis have so far correlated coding and a few non-coding variants in the region with LOXL1 expression levels, but functional effects of these variants is unclear. We hypothesize that analysis of the contribution of the genetically determined component of gene expression to XFS risk can provide a powerful method to elucidate potential roles of additional genes and clarify biology that underlie XFS.

Results Transcriptomic Wide Association Studies (TWAS) using PrediXcan models trained in 48 GTEx tissues leveraging on results from the multi-ethnic and European ancestry GWAS were performed. To eliminate the possibility of false-positive results due to Linkage Disequilibrium (LD) contamination, we i) performed PrediXcan analysis in reduced models removing variants in LD with LOXL1 missense variants associated with XFS, and variants in LOXL1 models in both multiethnic and European ancestry individuals, ii) conducted conditional analysis of the significant signals in European ancestry individuals, and iii) filtered signals based on correlated gene expression, LD and shared eQTLs, iv) conducted expression validation analysis in human iris tissues. We observed twenty-eight genes in chr15q22–25 region that showed statistically significant associations, which were whittled down to ten genes after statistical validations. In experimental analysis, mRNA transcript levels for ARID3B, CD276, LOXL1, NEO1, SCAMP2, and UBL7 were significantly decreased in iris tissues from XFS patients compared to control samples. TWAS genes for XFS were significantly enriched for genes associated with inflammatory conditions. We also observed a higher incidence of XFS comorbidity with inflammatory and connective tissue diseases.

Conclusion Our results implicate a role for connective tissues and inflammation pathways in the etiology of XFS. Targeting the inflammatory pathway may be a potential therapeutic option to reduce progression in XFS.

Keywords Exfoliation syndrome, GWAS, TWAS, transcriptomics, GTEx, predicted expressions

*Correspondence:

Jibril B. Hirbo

jibril.hirbo@vumc.org

Full list of author information is available at the end of the article



© The Author(s) 2023. **Open Access** This article is licensed under a Creative Commons Attribution 4.0 International License, which permits use, sharing, adaptation, distribution and reproduction in any medium or format, as long as you give appropriate credit to the original author(s) and the source, provide a link to the Creative Commons licence, and indicate if changes were made. The images or other third party material in this article are included in the article's Creative Commons licence, unless indicated otherwise in a credit line to the material. If material is not included in the article's Creative Commons licence and your intended use is not permitted by statutory regulation or exceeds the permitted use, you will need to obtain permission directly from the copyright holder. To view a copy of this licence, visit <http://creativecommons.org/licenses/by/4.0/>. The Creative Commons Public Domain Dedication waiver (<http://creativecommons.org/publicdomain/zero/1.0/>) applies to the data made available in this article, unless otherwise stated in a credit line to the data.

Introduction

Exfoliation syndrome (XFS) is an age-related systemic disorder characterized by excessive production and progressive accumulation of abnormal extracellular material, with pathognomonic ocular manifestations [1, 2]. The exact pathophysiological processes that underline XFS is still unclear. However exfoliative material typically builds up at the anterior part of the eye, including in and around the trabecular meshwork slowing aqueous humor outflow and causing elevation in intraocular pressure [3–5]. It is the most common cause of secondary glaucoma, resulting in widespread global blindness [6]. In addition to ocular manifestations, exfoliation syndrome deposits have been observed in visceral organs, such as the lung, kidney, liver and gallbladder [2, 7]. In addition to elastic tissue disorders, XFS has also been associated with increased risk of vascular diseases [8–10]. Associations of XFS to several systemic biomarkers of inflammation, including complement components and homocysteine, have also been reported [6, 11, 12].

Genetic mechanisms have substantial influence on XFS etiology as evidenced in family and twin studies [13, 14]. There have been eight genome-wide association studies (GWAS) of XFS [10, 15–20], three of which include meta-analysis [10, 15, 21], that have cumulatively identified >60 associated genetic variants. The largest meta-analysis of XFS involved >123,000 individuals (13,620 XFS cases, 109,837 controls) from 24 countries across six continents and identified seven loci with the strongest association signal in chromosome 15 near the *lysyl oxidase-like 1* gene (*LOXLI*) [15, 21], which encodes a member of family of proteins involved in formation of crosslinks in collagen and elastin [22]. The signal on chr15 involved 54 potential causal variants. Overall, (i) two missense variants in *LOXLI*, rs1048661 (encoding *LOXLI* p.Leu141Arg) and rs3825942 (p.Gly153Asp), are likely to confer risk of developing XFS, with very high heterogeneity across populations because the alleles show an effect reversal [15, 18, 21, 23–26], (ii) the associated variants in the locus showed population-specific frequency and LD patterns [15, 18, 21, 24], (iii) haplotypes that carry the risk alleles depending on the population are correlated with reduced *LOXLI* expression levels, however, (iv) no clear functional effects for the haplotypes that represent the two variants have been shown [10, 27, 28]. The non-coding variants associated with XFS at this chr15 locus could confer regulatory effects. Some of these non-coding variants regulate expressions of the sentinel *LOXLI* and the neighboring *STRA6* gene [10, 29, 30].

After considering all the reports on genetic architecture of XFS to date, we hypothesize that analysis of the

contribution of the genetically determined component of gene expression to XFS risk can provide a powerful method to elucidate potential roles of additional genes in XFS. We used a gene-based TWAS method, PrediXcan [31], implemented on GWAS summary statistics (Summary PrediXcan; S-PrediXcan) [32] to identify genetically determined gene expression traits associated with disease risk. Models were trained on 48 Genotype-Tissue Expression (GTEx ver. 8) project tissues: Adipose - Subcutaneous, Adipose - Visceral (Omentum), Adrenal Gland, Artery - Aorta, Artery - Coronary, Artery - Tibial, Brain - Amygdala, Brain - Anterior cingulate cortex (BA24), Brain - Caudate (basal ganglia), Brain - Cerebellar Hemisphere, Brain - Cerebellum, Brain - Cortex, Brain - Frontal Cortex (BA9), Brain - Hippocampus, Brain - Hypothalamus, Brain - Nucleus accumbens (basal ganglia), Brain - Putamen (basal ganglia), Brain - Spinal cord (cervical c-1), Brain - Substantia nigra, Breast - Mammary Tissue, Cells - Cultured fibroblasts, Cells - EBV-transformed lymphocytes, Colon - Sigmoid, Colon - Transverse, Esophagus - Gastroesophageal Junction, Esophagus - Mucosa, Esophagus - Muscularis, Heart - Atrial Appendage, Heart - Left Ventricle, Liver, Lung, Minor Salivary Gland, Muscle - Skeletal, Nerve - Tibial, Ovary, Pancreas, Pituitary, Prostate, Skin - Not Sun Exposed (Suprapubic), Skin - Sun Exposed (Lower leg), Small Intestine - Terminal Ileum, Spleen, Stomach, Testis, Thyroid, Uterus, Vagina, Whole Blood [33, 34]. GTEx is a comprehensive public resource to study tissue-specific gene expression and regulation [33, 34]. We estimated the correlation between genetically determined gene expression and XFS risk by leveraging on XFS GWAS summary statistics from a previously reported multi-ethnic study [21]. The phenomenon of TWAS association with multiple signals within the same locus can be a statistical artifact of the correlation due to LD between SNPs that are separately predictive of the measured expression of physically co-localized genes [35] hampering the ability to prioritize the true causal gene(s). To address this limitation, we performed sequential conditional analysis in each tissue, starting with the gene that was the strongest signal in the initial PrediXcan analysis. In addition, we sequentially rebuilt prediction models excluding variants in models of other genes in the loci that were in LD with any variants of the strongest signal. We also analyzed individual-level GWAS data from three additional European ancestry populations, German, Italian and American [10, 31]. We followed these extensive statistical analyses by functional validation in human iris tissues of the prioritized top gene-level associations. Finally, to gain clinical insights into our findings,

we explored the health consequences to individuals carrying high XFS genetic risk in a large biobank with links to electronic health records.

Results

PrediXcan analysis

We performed single-tissue PrediXcan analysis of the global multi-ethnic GWAS (13,620 XFS cases and 109,837 controls) summary data, identifying 23 genes (defined as signals with $P < 2.02 \times 10^{-7}$ after Bonferroni corrections) on chromosome 15: *CYP1A2*, *CYP1A1*, *STOML1*, *LOXLI*, *ISLR2*, *RPP25*, *INSYN*, *ISLR*, *STRA6*, *CD276*, *NEO1*, *ARID3B*, *COX5A*, *PML*, *CPLX3*, *LMAN1L*, *UBL7*, *MPI*, *CLK3*, *CSK*, *SEMA7A*, *TBC1D21*, and *NPTN* that mapped to region 15q22–25 region that spans ~3 Megabases (Fig. 1a, b and Suppl. Table S2).

To determine the joint effects of gene expression variation predicted across all 48 tissues analyzed, we performed a multivariate regression multi-tissue analysis. Each of the 23 associations from the single-tissue PrediXcan analysis remained significant in multi-tissue analysis (Suppl. Table S3). Additionally, five genes within the same region that were associated with XFS at subgenome-wide significance in the single-tissue analysis ($p < 3.02e-6$) were associated in the multi-tissue analysis: *ADPGK* ($p = 7.32E-07$), *CYP11A1* ($p = 1.36E-16$), *HEXA* ($p = 1.03E-06$), *PARP6* ($p = 1.82E-06$), *SCAMP2* ($p = 1.65E-10$) (Fig. 1b).

Seven additional genes located on chromosomes 1 (*LGR6* $p = 2.20E-06$; *SDHB* $p = 8.07E-08$), 6 (*PRRT1* $p = 9.10E-07$), 8 (*PRSS55* $p = 4.18E-13$), 10 (*CDH23* $p = 1.86E-07$; *PITRM1* $p = 8.45E-12$) and 19 (*CALM3* $p = 2.60E-07$), were significantly associated in the multi-tissues analysis (Fig. 1a, Suppl. Table S3). All seven signals mapped to genomic regions harboring GWAS SNP variants showing subgenome-wide significance with XFS risk, except for *PRRT1*, which corresponds to the *AGPAT1* GWAS locus [36]. The data indicates that combining information across variants in genes and then across tissue expression improves the power to identify

additional XFS-associated loci. To ensure that the association observed at the 23 genes from the larger multi-ethnic dataset was not an artefact of population structure, we confirmed the signals in a subset of European ancestry individuals (Materials and Methods, Suppl. Fig. S3, Suppl. Table S4, S5, S6).

Correlated expression among significant genes

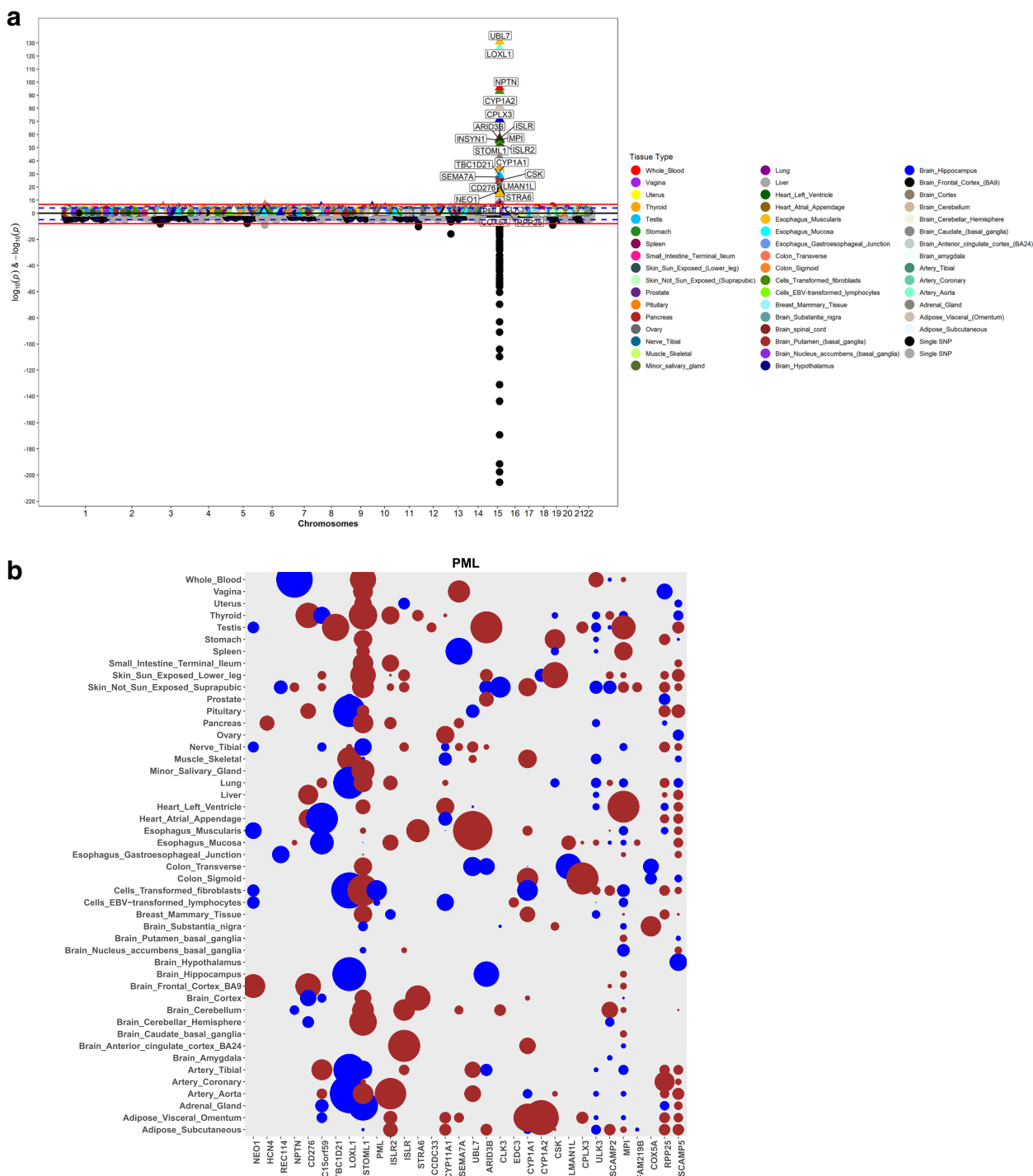
To determine whether the 23 observed association gene signals were artefacts of LD contamination, we calculated the pair-wise correlation in measured expression among the significant genes, using the reference GTEx panel. We further checked the relationship between expression correlation for each of the chr15p22–25 genes with *LOXLI* and *STOML1* and the PrediXcan associations for the two genes in each tissue. We made two important observations from this analysis. First, there was a significant correlation between the correlation of measured gene expression of the other genes in chr15p22–25 with *LOXLI* or *STOML1* and the gene-level associations with XFS in most tissues (Fig. 2e, f, Suppl. Fig. S4, Suppl. Table S7a). Secondly, there is substantial correlation between *STOML1* and *LOXLI* ($r^2 = 0.67$, $p = 0.009$) (Fig. 2e, f, Suppl. Fig. S4). These results indicate that the associations by one of the genes might be due to LD contamination or the presence of shared variants in the prediction models of the two genes (Fig. 2g, Table 2).

To dissect the potential source of LD contamination in the PrediXcan analysis, we looked into the effect of the two GWAS missense variants implicated in XFS that have mostly been linked to *LOXLI* and shown to play regulatory roles [27], followed by the effect of *LOXLI* and *STOML1* signals on chr15q22–25 region observed associations in each tissue. We also determined the effect of shared variants between prediction models for the genes in the region.

We modified our prediction models by excluding: i) rs3825942 missense variant, ii) rs4886776 intronic variant, which is at near perfect LD (pair-wise, $r^2 = 0.982$) with the rs1048661 missense variant, and iii) all the

(See figure on next page.)

Fig. 1 Manhattan plot for GWAS meta-analysis and PrediXcan analysis of the genotyping data for XFS. **a** The lower half of the plot is for the XFS meta-analysis summary statistics data Aung et al., 2017, while the upper half of the plot shows results from PrediXcan analysis for 48 GTEx tissues. On the X axis is plot of variant/gene associations along the chromosomes, while Y axis represent the significance levels for the associations. The legend for PrediXcan analysis on the 48 GTEx tissues, a color for each tissue, is on the right. For both plots the blue dotted line is the “suggestive” genome-wide significant threshold ($p < 1e-4$), while the red line is the genome-wide significant threshold. On the lower plot, the gene labels are for genes reported/mapped to genome-wide significant signals in GWAS result, while in the upper plot is for genes that are associated at genome-wide significant threshold. For genes associated with XFS at genome-wide threshold in more than one tissues, only the tissue with lowest p -value is labeled. The GWAS plot has been truncated to $p < 1e-220$ for clarity. **b** genes in the region in chromosome 15 that show significant association. The size of the balloon for each gene-tissue association is proportional to $-\log_{10} p_{\text{value}}$ and color corresponds to the predicted direction of expression changes: dark-red and blue for increased and decreased expression changes, respectively. Only four genes (*EDC3*, *ULK3*, *HCN4* & *FAM219B*) in the whole region were not associated with XFS



variants in our gene models that were in LD with the two variants ($r^2 > 0.1$). The two missense variants had wide ranging effect on the genetically predicted expression of many chr15q22–25 region genes, with the largest effect on *LOXL1*. The strength of the association signals

diminished in six of the nine tissues for which we had the gene’s predicted expression. Association signals in three of these tissues fell below genome-wide threshold in the global dataset (Suppl. Table S7b). In addition, association signals for seven additional genes in the region besides

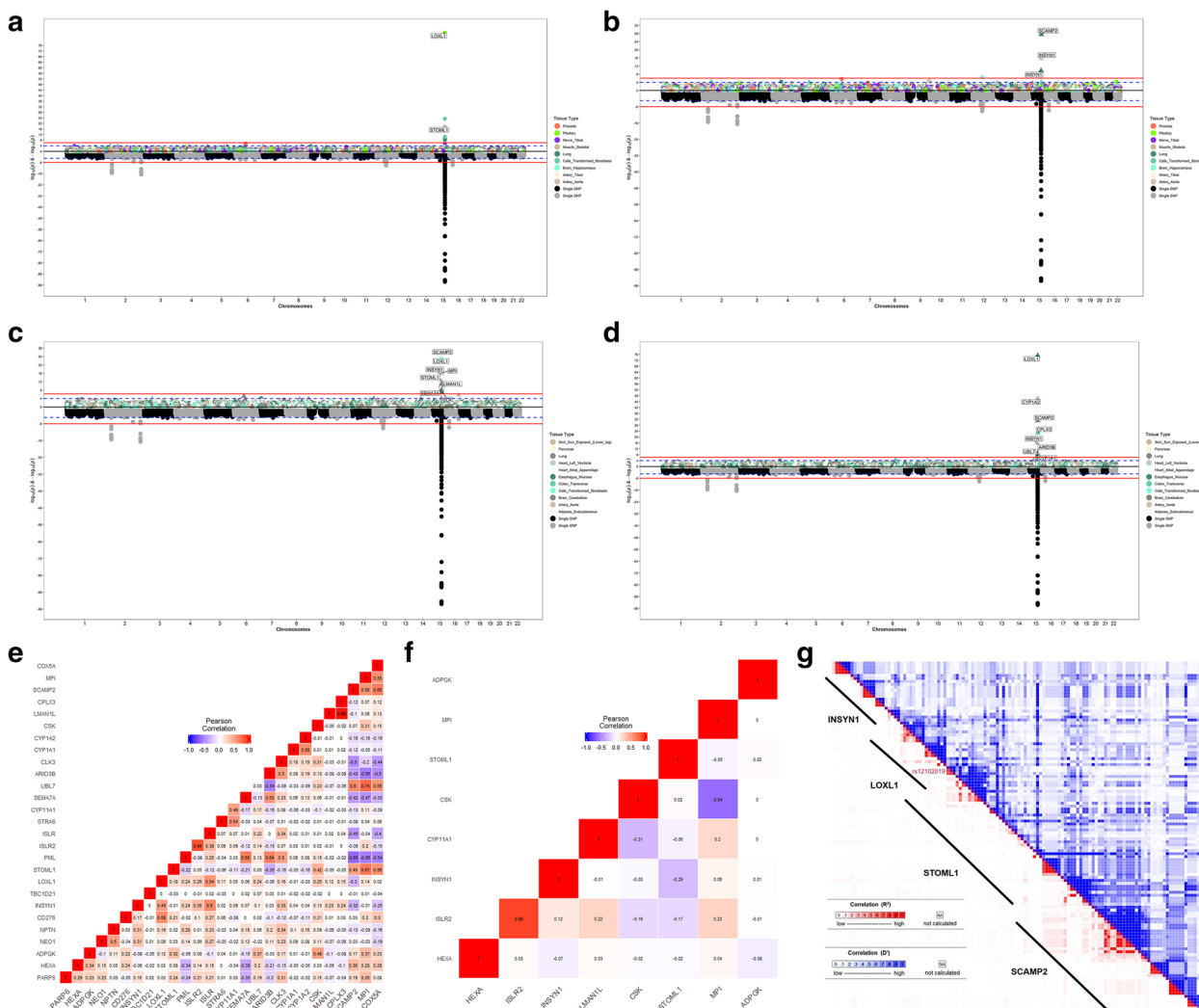


Fig. 2 Conditional analysis to prioritize XFS associated genes: a) Manhattan plot for PrediXcan analysis of European ancestry individuals in tissues with predicted gene expression for a) LOXL1 and b) conditioned on LOXL1 predicted gene expressions c) Manhattan plot for PrediXcan analysis of European ancestry individuals in tissues with predicted gene expression for STOML1 and d) conditioned on STOML1 predicted gene expressions e) correlation in gene expression in for genes in chr15q22–25 in lung tissue for i) reference GTEx data f) predicted gene expression in BioVU cohort. In each case on the X axis is plot of variant/gene associations along the chromosomes, while Y axis represent the significance levels for the associations. The legend for PrediXcan analysis on the GTEx tissues, a color for each tissue, is on the right. For both plots the blue dotted line is the “suggestive” genome-wide significant threshold ($p < 1e-4$), while the red line is the genome-wide significant threshold. On the lower plot, the gene labels are for genes reported/mapped to genome-wide significant signals in GWAS result, while in the upper plot is for genes that are associated at genome-wide significant threshold. For genes associated with XFS at genome-wide threshold in more than one tissues, only the tissue with lowest p-value is labeled. g linkage disequilibrium between variants in prediction models for LOXL1 and other chr15q22–25 genes associated with XFS in lung tissue based on pairwise r^2 and D' parameters. Relative genome location for variants in each gene models are roughly demarcated by diagonal lines next to gene symbols. Proximate location for the variant shared between LOXL1 and STOML1, rs12102019 is labelled

STOML1 lost genome-wide significance: *CD276* (2 tissues), *COX5A*, *CYP1A1*, *LMAN1L*, *MPI*, *SCAMP2* and *TBC1D21*.

Interestingly, association signals for eight genes were strengthened, four of which attained genome-wide significance threshold in reduced models: *INSYNI*, *CYP1A1*, *NPTN* and *LOXL1* (Suppl. Table S7b). These shifts in association strength, i.e., an increase in effect size, seem

to be due to the exclusion of select variants (Suppl. Tables S7c, S7d). Moreover, the shifts in association strength are correlated with the excluded variants’ level of LD with the missense variant rs3825942 ($r^2 = 0.64$) (Suppl. Tables S7c, S7d). Notably, the three GWAS variants identified to have effect reversal in South Africans relative to other populations were in high LD with rs3825942 (Suppl. Table S7g) [21]. Our results indicate that the missense variants have

enhancing or diminishing effects on the PrediXcan association signals, in chr15q22–25, with XFS, consistent with allele reversal reported for the GWAS variants [36].

To check whether the association signals in the chr15q22–25 region for each tissue were independent of the ‘sentinel’ *LOXLI* signal, we excluded, from the prediction models, variants that were in LD ($r^2 > 0.1$) with any variants in *LOXLI* or *STOML1* tissue models. We also excluded variants that were shared between two or more genes in their original prediction models. Seven of the genes that were associated with XFS at genome-wide threshold in their original models showed diminished signals, including four below significance levels: *UBL7*, *ISLR*, *LMAN1L* and *COX5A* in reduced models (Suppl. Table S7e). Association signals for *CYP1A1* and *CYP1A2* were slightly diminished in reduced models relative to the original models, but remained at significant genome-wide thresholds (Suppl. Table S7e). However, association signals for six genes strengthened, four of which attained genome-wide association significance levels in the reduced models: *INSYNI*, *CLK3*, *CYP1A1* and *NEO1* (Suppl. Table S7e). These shifts in association strength seem to be due to few variants that are either in LD with variants in *LOXLI* and *STOML1* models or are shared with other genes’ models (Suppl. Tables S7e, S7f). However, these variants causing the shifts in association signals upon exclusion from the models, were not in LD with the missense rs3825942 variant (Suppl. Table S7g). This indicates that there are signals of allele reversal independent of the known missense variants in *LOXLI*.

Excluding variants that are in LD with SNPs in the *LOXLI/STOML1* models did not have any effect on the association signals for six genes that were associated with XFS at genome-wide threshold in the original models: *CSK*, *STRA6*, *CD276*, *ARID3B*, *MPI* & *TBC1D21*, with the latter three in testis, for which we had no models for both *LOXLI* and *STOML1* (Suppl. Table S7e). The results indicate that some of the observed signals were artefacts of LD contamination from *LOXLI* and *STOML1* (*ISLR*, *LMAN1L* and *COX5A*), while some of the signals were masked in the original models (*INSYNI*, *CLK3*, *CYP1A1* and *NEO1*). There was inconsistent result for *UBL7*, where there was no effect in its association signal in a tissue, enhanced effect in another tissue, and diminished signal in two other tissues, one of which went below the genome-wide threshold, albeit the reduced model had only a single variant in the prediction (Suppl. Table S7e).

Conditional analysis

Conditional analysis was performed in tissues with any genome-wide significant chr15p22–25 region gene signals against the predicted gene expression for the strongest observed signals in the European subset. As in the

global dataset, the strongest signals in the European dataset were at *LOXLI* (Table 1, Suppl. Fig. S3). In all nine of the 48 tissues with *LOXLI* predicted expression, only the *STOML1* gene showed a significant association signal (in addition to *LOXLI*) (Table 1, Suppl. Fig. S3). After conditioning on *LOXLI* in these tissues, the *STOML1* signal disappeared, but association signals at *SCAMP2* and *INSYNI* were observed in artery-aorta and lung tissues, respectively (Fig. 2a, b, Suppl. Table S8). This indicated that the association of *STOML1* with XFS is an artefact of a strong *LOXLI* signal, consistent with *LOXLI* being the true signal and *STOML1* a proxy signal. In addition, association signals for *SCAMP2* and *INSYNI* were masked by the *LOXLI* signal.

In 17 tissues with *STOML1* predicted gene expression, we observed significant association signals for 8 other genes (in addition to *STOML1*) (Fig. 2c, d, Suppl. Table S8). After conditioning on *STOML1* predicted gene expression, associations with four genes (*CYP1A1*, *INSYNI*, *LOXLI*, *SCAMP2*) remained, while association with four other genes (*ISLR*, *LMAN1L*, *MPI* & *SEMA7A*) disappeared. In addition, associations with five more genes (*ARID3B*, *CPLX3*, *CYP1A2*, *PML* & *UBL7*) attained genome-wide significance after the conditional analysis.

Overall, conditional PrediXcan analysis of genetic signals in the chromosome 15 region in the European

Table 1 Genes associated with XFS and replicated in European Ancestry individuals

Chromosome	Genes associated with XFS
chr1	^a LGR6; ^a SDHB
chr6	^a PRRT1
chr8	^a PRSS55
chr10	PITRM1*; ^a CDH23
chr11	^a TMEM136
chr15	SEMA7A***;STOML1***;ADPGK;MPI***;HEXA*; ^a LOXLI***;CPLX3*; ^a INSYNI***;SCAMP5**; ^a ISLR***;CYP11A1*; ^a NPTN*; ^a CSK**; ^a NEO1*; ^a UBL7***;CD276**; ^a STRA6**; ^a PARP6*; ^a LMAN1L***; ^a ISLR2*; ^a ARID3B*; ^a LK3*; ^a PML*; ^a SCAMP2***; ^a TBC1D21; ^a CYP1A2*; ^a CYP1A1***; ^a RPP25; ^b ULK3**
chr16	^b CDYL2**
chr19	^a CALM3

Gene associated with XFS in single tissues analysis at genome-wide significance threshold (< 2.02e-7) in global GWAS summary statistic

Gene associated with XFS in cross-tissue analysis (< 9.5e-6) and in single tissues analysis at suggestive significance threshold (< 1e-4) in global GWAS summary statistics

Significance values in European ancestry data single tissue analysis of genes associated with XFS ***p value < 2.02e7, ** p value < 1e-4, * p value < 0.05

^a genes associated with XFS in global dataset but with no association signals in European ancestry data at even nominal threshold (< 0.05)

^b Additional genes associated with XFS in cross-tissue analysis of European ancestry data but not in global dataset

dataset in a limited number of tissues was mostly consistent with PrediXcan analysis using the reduced models above. The analysis confirms the associations for *LOXLI*, *ARID3B*, *CPLX3*, *CYP1A1*, *CYP1A2*, *INSYNI*, *NEO1*, *PML*, *SCAMP2*, and *UBL7*, all of which, except for *INSYNI*, have been shown to be highly expressed in eye tissues [37] (Suppl. Fig. S5). However, *INSYNI* has enhanced expression in brain tissues [38, 39]. Collectively, these results suggest that some of the identified gene-level association signals between XFS and genetically imputed expression were driven by correlation to the strong *LOXLI* and its “proxy” *STOML1* signal.

Enrichment and pathway analysis

Genes at genome-wide significance ($p < 2.02e-7$) and nominal significance ($p < 0.05$) were evaluated for enrichment of known pathways, using Enrichr [40, 41]. Genes at genome-wide significance were enriched for genes reported for, or mapped to, GWAS variants implicated in several caffeine-related (coffee and caffeine consumption, and caffeine metabolism [42–44]) and blood pressure [45] traits. The enrichment for coffee consumption is replicated for the larger gene set that is associated with XFS at nominal significance [36]. Some of these genes, *CYP1A1* and *CYP1A2* [46], are involved in fatty acid oxidation and estrogen receptor pathways. In addition, these two genes are also observed in the Reactome enrichment of protectin synthesis (Table 2, Suppl. Table S9).

Our gene set is also enriched for genes associated with carcinoma and three inflammatory conditions: rheumatoid arthritis, Type 1 diabetes, vitiligo in Jensen Diseases,

a database that integrates evidence on disease-gene associations from automatic text mining, manually curated literature, cancer mutation data, and GWAS (<https://diseases.jensenlab.org/>).

We further analyzed our gene list against compounds in Drug Signatures Database (DSigDB, <http://tanlab.ucdenver.edu/DSigDB>), a gene set resource that relates drugs/compounds and their target genes. Our gene set is enriched for genes that are targets of cyclosporin A ($p = 9.66E-11$), and genes that are targets for compounds that are either 1) carcinogenic: Aflatoxin B1, potassium chromate, methyl methanesulfonate and copper sulfate, 2) neuroactive: valproic acid and methamphetamine, 3) neuroprotective: quercetin and epigallocatechin gallate, or 4) analgesic: acetaminophen (Table 2, Suppl. Table S9). Cyclosporin A is an immunosuppressant taken to treat rheumatoid arthritis and other autoimmune conditions, while quercetin and acetaminophen have been shown to have anti-inflammatory effects [47, 48].

Analysis in Gene Set Enrichment Analysis (GSEA) using a ranked association gene list based on effect sizes confirmed some of the enrichment observations using Enrichr. GSEA besides replicating enrichment for acetaminophen, showed enrichment for: 1) six synthetic estrogens, 2) estrogen regulators (Clomifene), 3) antiarrhythmic (quinidine), and 4) an anti-fungal (ketoconazole) (Table 2, Suppl. Table S9). The gene set was also enriched for genes that were associated with the collagen fibril crosslinking (FDR=0.0313) Reactome pathway. Analysis of the gene list in relation to the latest Reactome library (<https://reactome.org/>) returned

Table 2 Enrichment analysis of genes that are associated with XFS

Tool	Database	enrichment	Name	# found	# total	Adj-p-values/FDR
Reactome	reactome	pathway	Endosomal/Vacuolar pathway	59	82	1.83E-07
GSEA	reactome	pathway	Crosslinking of collagen fibrils	5	8	0.031
Enrichr	Jensen Diseases	Disease	Rheumatoid_arthritis	119	310	8.32E-08
			Type_1_diabetes_mellitus	68	158	.69E-06
			Carcinoma	2619	11,318	0.013
			Vitiligo	28	63	0.029
Enrichr	GWAS Catalog	traits	Caffeine consumption	11	14	0.019
Enrichr	DSigDB	Drugs	cyclosporin A_CTD_00007121	1258	4826	9.66E-11
			VALPROIC ACID_CTD_00006977	2041	8313	1.75E-09
			Copper sulfate_CTD_00007279	1508	6017	3.04E-08
			quercetin_CTD_00006679	812	3159	7.82E-05
			acetaminophen_CTD_00005295	1017	4136	0.007
			AFLATOXIN B1_CTD_00007128	773	3082	0.006
			(-)-Epigallocatechin gallate_CTD_00002033	546	2115	0.005
			POTASSIUM CHROMATE_CTD_00001284	491	1898	0.011
			METHAMPHETAMINE_CTD_00006286	40	102	0.030
			METHYL METHANESULFONATE_CTD_00006307	940	3685	0.047

significant enrichment for the endosomal-vacuolar pathway ($p=8.14E-11$), an enrichment that was replicated in gene sets that were predicted to be downregulated ($p=3.24E-8$). Our results broadly recapitulated results above, even after excluding genes in HLA and chr17 inversion regions from the enrichment analysis of the gene set ($p < 0.05$) (Table 2, Suppl. Table S9).

Quantitative expression validation analysis

Expression levels of *ARID3B*, *CD276*, *INSYNI*, *LOXL1*, *NEO1*, *SCAMP2*, *STOML1* and *UBL7* were measured in XFS ($N=12$) and control ($N=19$) eye tissues. We selected iris tissue because it is one of the tissues that are part of the anterior segment structures bathed by aqueous humor and upon which the flaky XFS materials are deposited [3–5]. Other affected structures include the trabecular meshwork, lens capsule, ciliary body, zonules and corneal endothelium [3–5]. All transcript levels were found to be decreased in iris tissues obtained from XFS patients compared to control samples, with significant differences for *ARID3B*, *CD276*, *LOXL1*, *NEO1*, *SCAMP2* and *UBL7* ($p < 0.05$) (Fig. 3). *INSYNI* and *STOML1* were not significantly downregulated in diseased eyes relative to normal eyes in validation analysis. *STOML1* is the closest gene to and potentially proxy for *LOXL1* among those that show association in our PrediXcan results within the chr15q22–25 region. We included it as a negative control in the validation analysis, while *LOXL1* was a positive control considering that it had already been

shown to exhibit pattern of downregulation in gene expression in diseased relative to normal tissues [36]. *CD276* was selected for functional validation in eye tissue despite no significant association with XFS in single-tissue analysis in the European ancestry data because it was significantly associated with XFS in multi-tissue analysis in European data. In addition, it was one of the gene associations signals which were not affected by excluding variants that were in LD with *LOXL1/STOML1* model SNPs in the multi-ethnic global dataset. Overall, our validation results replicate the associations found using the genetically determined gene expression.

Comorbidity/pleiotropy analysis

To gain further biological insights into the gene associations we observed in our PrediXcan analysis, we performed logistic regression analysis of both XFS ICD9/10 diagnosis, and Polygenic Risk Score generated from the multi-ethnic summary data across the BioVU individuals, Vanderbilt University's electronic health records database linked to genetic information, as the target dataset (Materials and Methods). XFS diagnosis was associated with an increased risk of 96 phenotypes in BioVU, including 12 musculoskeletal phenotypes, 4 infectious diseases, and 1 cardiovascular phenotype. These results are consistent with higher comorbidity of diseases affecting inflammation, connective tissue, and the circulatory system in individuals with XFS (Suppl. Fig. S6a, Suppl. Table S10a).

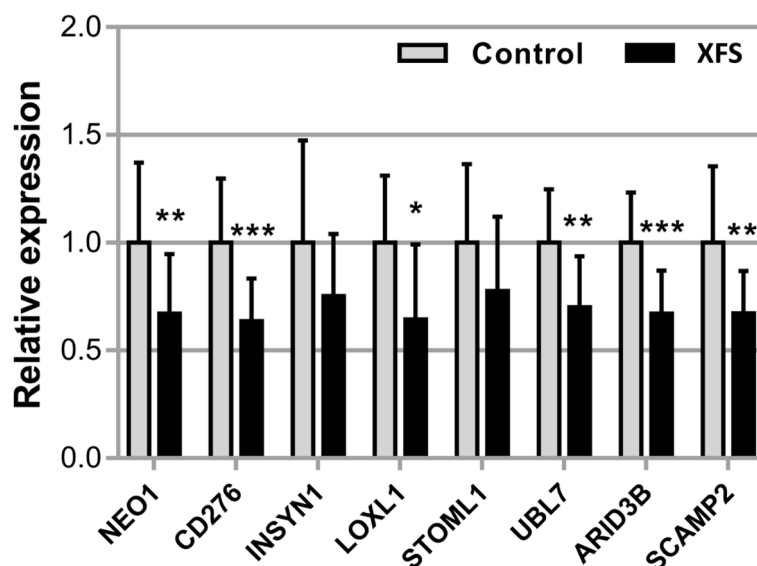


Fig. 3 Expression of *NEO1*, *CD276*, *INSYNI*, *LOXL1*, *STOML1*, *UBL7*, *ARID3B* and *SCAMP2* mRNA in iris tissues derived from normal human donors (control) ($n = 19$) and donors with XFS syndrome ($n = 12$) using real-time PCR technology. Expression levels were reduced in XFS specimens compared to control specimens, with significant differences for *NEO1*, *CD276*, *LOXL1*, *UBL7*, *ARID3B* and *SCAMP2*. The relative expression levels were normalized relative to GAPDH and are represented as mean values \pm SD (* $p < 0.05$; ** $p < 0.01$; *** $p < 0.001$)

XFS polygenic score was not significantly associated with any phenotypes in the analysis (Suppl. Fig. S6b). This potentially indicated that PRS generated from the global multi-ethnic GWAS summary might not be powered to detect association with traits in the EHR, and we might require scores from a more homogeneous and a much larger sample size. However, among the top PRS associations, we found several inflammatory diseases (Suppl. Table S10b), consistent with the enrichment results reported above.

Discussion

We performed gene-based association analysis using GWAS summary statistics and conducted extensive statistical validation of genes associated with XFS. From our PrediXcan analysis, we identified 35 associated genes with XFS, 23 in single-tissue analysis and the rest in multi-tissue analysis. To eliminate the possibility of false-positive results due to LD contamination, we performed extensive additional analyses. First, we performed PrediXcan analysis in reduced models removing variants in LD with the two *LOXLI* missense variants associated with XFS, and variants in *LOXLI/STOML1* models in both global multiethnic and a subset of European ancestry individuals. Secondly, we conducted conditional analysis of the significant signals in European ancestry individuals. Thirdly, we then filtered signals based on correlated gene expression, LD and shared eQTLs and confirmed thirteen genes to be associated with XFS. Finally, expression analysis in human iris tissues further confirmed six of these seven signals, which were significantly downregulated in diseased XFS relative to normal eye tissues: *ARID3B*, *CD276*, *LOXLI*, *NEO1*, *SCAMP2* and *UBL7*.

Our results suggest potentially substantial roles of inflammation and environment in the etiology of XFS. All the six genes prioritized here by prediction and extensive validation analyses have inflammatory roles. *ARID3B*, *CD276*, *LOXLI* and *NEO1* are immunoregulatory molecules involved in the interaction between different tumors and the immune system [49–52]. *SCAMP2* is important in granule exocytosis, a process crucial in membrane fusion in normal cellular functions in diverse systems including the immune system's inflammatory response [53–55]. *CD276* is involved in regulation of Ag-specific T cell-mediated immune responses and participates in the innate immunity-associated inflammatory response [56, 57]. *LOXLI* has also been implicated in fibrosis in response to inflammation in human breast cancer [36], in liver and lungs in model animals [36, 36,36]. *UBL7* encodes a member of the ubiquitin protein family, that is crucial in immune response and regulation of inflammatory response [58–60].

Genes that show significant association of predicted expression with XFS at nominal significance are enriched for genes associated with three inflammatory conditions: rheumatoid arthritis, Type 1 diabetes and vitiligo in the Jensen Diseases database, with genes associated with the former two conditions enriched even with HLA region excluded. This is also consistent with the enrichment we find in DSigDB and DrugBank for cyclosporin A, acetaminophen and quercetin, which are compounds that have anti-inflammatory effects [61].

Enrichment of predicted genes in this study in the polyunsaturated fatty acid (PUFA) and steroid derivatives: protectin (Reactome), omega fatty acid and estrogen (WikiPathways) are also consistent with the potential role of inflammation in XFS. Protectin, a derivative of PUFA including Omega-3 that are major components of fish oil, has an anti-inflammatory, anti-amyloidogenic, and anti-apoptotic activities in human neural cells [36, 62, 63]. Omega fatty acid has been suggested as an IOP reducing supplement [36, 64, 65] because of its anti-inflammatory effects [66]. Association of steroid derivative estrogen with glaucoma has been previously explored with higher levels of estrogen in reduction in IOP and conferring a possible reduced risk of glaucoma [67]. The synthetic form of estrogen, estradiol, has been shown in a rat glaucoma model to inhibit optic nerve axonal degeneration by inducing a protein that is crucial in protecting RGC from oxidative damage [68, 69].

The association with inflammation is consistent with studies in limited numbers of XFS patients that found elevated inflammatory markers relative to controls, including cytokines, and markers such as interleukin-6 (*IL-6*) and *IL-8* [70, 71], tumor necrosis factor- α (*TNF- α*) and *YKL-40* [72, 73]. However, there are conflicting results for high sensitivity C-reactive protein [74, 75].

In addition, the XFS gene sets are enriched for genes that map to variants implicated in coffee and caffeine intake. Effects of caffeine consumption in the etiology of XFS have been studied, on the premise that coffee consumption increases plasma homocysteine levels that are speculated to enhance XFS material formation by contributing to vascular damage, oxidative stress, and extracellular matrix alterations [36, 76–78]. Consumption of coffee has been reported to have both pro- and anti-inflammatory effects [79]. However, review of fifteen studies on the effect of coffee and caffeine on inflammation inferred the former had anti-inflammatory action, while the latter had complex effects on the inflammatory response with both proinflammatory and anti-inflammatory responses reported [36]. Caffeine might have a neuroprotective role by regulating pathways that produce inflammatory molecules via adenosine receptors in brain cells [80, 81]. Posttranscriptional regulation of *LOXLI*

gene expression has been also shown to be modulated by caffeine [82].

Globally, our results of the six novel functionally validated genes also confirm the role of connective tissue involvement in the etiology of XFS. Aung, et al. [36], demonstrated the role of haplotypes that carry *LOXLI* XFS causal coding variants in upregulating extracellular matrix components such as elastin and fibrillin, and increasing cell-cell adhesion. In addition, two of the novel genes in our study, *ARID3B* and *NEO1*, among the other six genes identified and validated in both studies, have adhesive roles in the body. *ARID3B* in conjunction with *FDZ5* protein increases adhesion to ECM components, collagen IV, fibronectin and vitronectin, that are components of exfoliation deposits [83, 84]. *NEO1* has also been shown to play adhesive role during organogenesis [85].

Results from our enrichment analysis of genes associated with XFS are also consistent with a role of dysregulation in connective tissue metabolism in the etiology of XFS. Cyclosporin_A regulate *lysyl oxidase* expression and collagen metabolism probably by inhibiting an isomerase involved in protein folding [36, 86, 87]. Other anti-inflammatory compounds identified from our enrichment analysis in the current study, epigallocatechin gallate, valproic acid, quercetin, ketoconazole and acetaminophen have also been shown to suppress collagen and/or are anti-fibrotic in variety of tissues by yet to be elucidated mechanism [88–92]. Moreover, coffee and caffeine inhibit collagen expression and deposition, and have anti-fibrotic effects by blocking expressions and/or by modulating effects of profibrotic factors [93–96].

Our results that show enrichment in crosslinking of collagen fibrils, a crucial constituent of connective tissues, and endosomal-vacuolar Reactome pathways, in our associated genes further confirm the importance of connective tissues in the etiology of XFS. In addition, there may be anomalies in an endosomal-vacuolar pathway shown to be involved in the accumulation of other aberrant proteins, including: A β peptides [97], prion [98], and Huntingtin [99] in neurons, and implicated in neurodegeneration. Moreover, inflammation has also been suggested in migratory failure and subsequent deposition of aberrant proteinaceous materials in affected tissues in conjunction with other molecular actors [71, 100–105].

Finally, our comorbidity analysis in the BioVU EHR indicated XFS association with several chronic inflammatory dermatological, musculo-skeletal, respiratory, and infectious conditions. Moreover, extracellular matrix dysregulation is also suggested by our PheWAS results indicating XFS comorbidity with Vitamin D deficiency. Vitamin D regulate collagen cross-linking in vitro by upregulating gene expression of specific lysyl hydroxylase and oxidase enzymes [36].

Limitations of the study

This study has two main limitations. First, even though GTEx data for the 48 tissues represent the most comprehensive eQTL data set of human tissues, it does not constitute a complete representation of all human tissues and may fail to identify the real causal genes in the unsampled ocular tissue. However, we have confirmed from an ocular tissue database that novel signals identified in this study are robustly expressed in XFS relevant eye tissues. Moreover, recent analysis shows that the majority of the human body tissues exhibit higher degrees of tissue similarities [106]. In addition, it has been shown that most complex conditions, including XFS, might actually manifest in many diverse tissues in the body [106].

Second, only a third of the signals identified in the larger data were robustly confirmed in a European dataset at genome-wide significance. This raised the possibility that most of the initial signals identified an artefact of local LD leakage or shared eQTLs with the sentinel *LOXLI/STOML1* signal. Using statistical validation with reduced models including no SNPs in LD with sentinel variants, we confirmed associations independent of *LOXLI* for at least ten genes including seven that were experimentally validated. In addition, results from a recent study are consistent with two other association gene signals confirmed using multi-tissue analysis of European dataset and PrediXcan of reduced models in multi-ethnic global data, *ISLR2* and *STRA6* [29]. *ISLR2* and *STRA6* are both significantly downregulated in tissues of XFS patients together with other key components of the *STRA6* receptor-driven Retinoic acid (RA) signaling pathway, and that siRNA-mediated downregulation of RA signaling induces upregulation of *LOXLI* and XFS-associated matrix genes in XFS-relevant cell types [29]. These data indicate that dysregulation of *STRA6* and impaired retinoid metabolism are involved in the pathophysiology of XFS syndrome. Retinoic acid, the active metabolite involved in the signaling pathway implicated by Berner et al. [29] in XFS through regulation of *ISLR2*, *STRA6* and *LOXLI*, has been shown to control critical checkpoints in inflammation and to promote an inflammatory environment [107–109].

Conclusions

Our analysis of predicted gene expression and extensive functional analysis in eye tissue prioritized six genes in association with XFS. Our results further confirmed the role of connective tissues and highlighted the importance of inflammation in the etiology of XFS. Thus, molecular elements that underlie the interaction of connective tissue biosynthesis and inflammatory pathways may play a central role in the etiology of XFS. Targeting the

inflammatory pathway may be a potential therapeutic option to reduce progression in XFS.

Materials and methods

We used an extension of PrediXcan [36] that uses GWAS summary statistics, S-PrediXcan [11], to analyze GWAS summary statistical data from a multi-ethnic GWAS study on XFS [36]. This dataset consisted of 13,620 XFS cases and 109,837 controls. We also performed PrediXcan on individual-level genetic data from two independent datasets comprising 4127 cases and 9075 controls. The first dataset comprised case and control samples from two cohorts of European ancestry (from Germany and Italy). The second dataset comprised adult patients of European ancestry at Vanderbilt University Medical Center (VUMC) from the local communities surrounding Nashville, TN. The BioVU cases and controls were genotyped on five different Illumina genotyping arrays; Human660W-Quad, HumanOmni1-Quad, Infinium Omni5-4, OmniExpress-8v1-2-B and Infinium Multi-Ethnic Global-8 (MEGA). The data was processed using established GWAS quality control procedures [8] and imputed on the Michigan Imputation server. Details on how subject selection for BioVU data and genotyping was performed is found in extended materials and methods section (Supplemental Information, Suppl. Fig. S1, S2).

Statistical analysis

We used the gene-based method, PrediXcan, that provides a framework for correlating imputed gene expression with phenotype [9]. Gene expression prediction models for 48 different human tissues were trained using GTEx ver. 8 data, subsampled to use only the European ancestry samples. Models with non-zero weights that met a set significance criterion ($r > 0.10$, $q < 0.05$) were retained [31]. Given the lack of eye tissue in the GTEx data, we performed PrediXcan analysis in all available tissues to leverage the shared regulatory architecture of gene expression across tissues [110]. We referred to the association analysis in each tissue between predicted expression and XFS as “single-tissue analysis.” Because XFS is considered a systemic disorder, we also aggregated evidence across the different tissues to improve our ability to prioritize genes relative to a single unrelated tissue. We determined the joint effects of gene expression variation predicted across all 48 tissues using the Multi-Tissue PrediXcan (MultiXcan), a multivariate regression method that integrates evidence across multiple tissues taking into account the correlation between the tissues [32, 34]. We refer to this association analysis as “multi-tissue analysis.”

We used S-PrediXcan [36] to analyze GWAS summary statistic data from the multi-ethnic study of Aung, et al.

[36]. Since the summary-based method has been shown to be conservative and tends to underestimate significance in cases where there is some linkage disequilibrium-structure mismatch between reference and study cohorts [36], we retained and reported S-PrediXcan results that had a univariate S-PrediXcan $P < 0.0001$. We used Bonferroni adjustment for multiple hypothesis testing. Genome-wide significance for a gene-level association in single-tissue and multi-tissue PrediXcan analysis were defined as $p < 2.02e-7$ and $p < 3.02e-6$, respectively.

Conditional analysis and linkage disequilibrium evaluation

To determine whether multiple association signals within the same locus are due to independent causal genes or statistical artefacts of correlation in measured expression and predicted gene expression for adjacent genes [35], we examined the correlation in the gene expression among genome-wide significant genes in the reference GTEx data. We assumed that there is concordance in correlation in measured and predicted gene expressions, but depending on the quality of our predictions, correlation in predicted expression for a pair of genes may be missed. We verified the extent of LD in the 1000 genomes database [111, 112] between variants in the prediction models for significantly associated genes in each tissue.

To measure potential regulatory effects of the two classical *LOXLI* missense variants in our PrediXcan analysis, we excluded them and all the variants in our gene models that were in LD with them (defined as pairwise $r^2 > 0.1$) to generate “reduced models.” We predicted gene expression and performed association analysis using reduced models in both the global multiethnic and the European subset for the genes in chromosome 15 region. To assess whether the association signals in the chr15q22–25 region for each tissue are independent of the ‘classical’ *LOXLI* signal, we excluded variants in the prediction models of genes in the region that were in LD (pairwise $r^2 > 0.1$) with any variant in the *LOXLI* model. In tissues without a *LOXLI* model (i.e., $r^2 > 0.10$, $q < 0.05$), we excluded variants for chr15q22–25 region genes that were in LD ($r^2 > 0.1$) with variants in the *STOML1* models. In addition, we excluded variants that were shared between prediction models for genes in the region. In each case, we performed association analysis using the reduced models and compared the results with the original models.

To determine whether additional genes within the region were significantly associated with XFS, independently of the most highly associated genes (*LOXLI* and *STOML1*) identified in the primary analysis, we performed conditional analysis using ancestrally ‘homogenous’ individual-level genotype data that included our BioVU cohort and a subset of Aung,

et al. consisting of three European ancestry cohorts. For each tissue with a significant association, the conditional analysis was performed on the gene that was the most statistically significant as identified from the initial PrediXcan analysis. We generated genetically determined expression for each individual in the dataset and then performed association analysis using Genetic Association Analysis Under Complex Survey Sampling (SUGEN: version 8.8) [113] on the individual imputed gene expression data, including age, sex, first 5 principal components and relatedness in the regression model. A new logistic regression model was then fit to the case-control data by sequentially adjusting for the expression data of the top significant signals as a covariate. We then performed a meta-analysis for the PrediXcan summary statistics from the four datasets. We repeated this procedure until no genes in the region attained our threshold for statistical significance in the tissues tested ($< 0.05/\text{total \# of e-genes} \times \#$ of tissues tested for each top round of tests).

Enrichment and pathway analysis

Genes that were predicted to be associated with XFS at genome-wide significance in both single-tissue and multi-tissue analysis, and at nominal significance ($p < 0.05$) in single-tissue analysis were checked for enrichment of particular categories in several databases using the web-based enrichment tools, Enrichr [40, 41]. This was done by using the strongest signal at nominal significance across the 48 tissues for each of the genes analyzed in PrediXcan. Enrichr implements Fisher's exact test and uses over 100 gene set libraries to compute enrichment [40]. We also performed rank-based Gene Set Enrichment Analysis (GSEA) using another web-based enrichment tool, 2019 Webgestalt [114–117] with a more recent database (Gene Ontology January 2019, KEGG Release 88.2, Reactome ver.66 September 2018 and PANTHER v3.6.1 Jan 2018) and the current Reactome database ver. 69 (June 12 2019) [118]. In this case the strongest signal in the PrediXcan result across the 48 tissues for each of the genes analyzed was used. Based on previous studies indicating limitation in accurately quantifying expression effects of variants in highly polymorphic regions [119, 120], we also performed enrichment analysis after excluding a total of 310 genes in ~6Mb chromosomes 6 HLA region (hg19 28Mb–34Mb) that encompassed *GPX6* – *CUTA* genes (238 genes) and ~2.5Mb chromosome 17 region that encompassed *CCDC43* – *NPPEPS* that include the 900kb inversion common in population of European ancestries (72 genes).

Quantitative expression validation analysis

Human tissues

Human donor eyes from European ancestry individuals used for corneal transplantation were processed within 20 hours after death with appropriate research consent obtained from the donors or from relatives for those who are deceased [29]. The procedure of the study was approved by the Ethics Committee of the Medical Faculty of the Friedrich-Alexander-Universität Erlangen-Nürnberg (No. 4218-CH) and consistent with the tenets of the Declaration of Helsinki [29].

For RNA and DNA extractions, 12 donor eyes with manifest XFS syndrome (mean age, 77 ± 9 years) and 19 normal-appearing control eyes without any known ocular disease (mean age, 74 ± 6 years) were used. All XFS tissues donors were previously confirmed XFS patients based on routine ophthalmologic examination after pupillary dilation. The presence of characteristic XFS material deposits was assessed by macroscopic inspection of anterior segment structures and confirmed by electron microscopic analysis of small tissue sectors. Iris tissues were prepared under a dissecting microscope and frozen rapidly in liquid nitrogen.

Real-time PCR

For quantitative real-time PCR, iris tissues ($N = 31$, 12 XFS and 19 control eyes) were extracted using the Precellys 24 homogenizer and lysing kit (Bertin, Montigny-le-Bretonneux, France) together with the AllPrep DNA/RNA kit (Qiagen, Hilden, Germany) according to the manufacturer's instructions including an on-column DNaseI digestion step using the RNase-free DNase Set (Qiagen). First-strand cDNA synthesis and PCR reaction was performed as previously described [36]. Exon-spanning primers (Eurofins Genomics, Ebersberg, Germany), designed with Primer 3 software (<http://bioinfo.ut.ee/primer3/>), are summarized in Suppl. Table S1. Quantitative real-time PCR was performed using the CFX Connect thermal cycler and software (Bio-Rad Laboratories, München, Germany). Probes were run in parallel and analysed with the $\Delta\Delta C_t$ method. Averaged data represent at least three biological replicates. Unique binding was determined with UCSC BLAST search (<https://genome.ucsc.edu/>) and amplification specificity was checked using melt curve, agarose gel and sequence analyses with the Prism 3100 DNA-sequencer (Applied Biosystems, Foster City, CA). For normalization of gene expression levels, mRNA ratios relative to the house-keeping gene GAPDH were calculated.

Group comparisons were performed using a Mann-Whitney U test using SPSS v.20 software (IBM, Ehningen, Germany). $P < 0.05$ was considered statistically significant.

Testing for comorbidity/pleiotropy

To determine the comprehensive health consequences of high genetic risk to XFS, we performed a phenome-wide association analysis (PheWAS) [121]. First, we examined the comorbidity of other phecodes with XFS (365.5 – ICD9 365.52/ICD10 H40.14xx) in a total of 752,024 individuals in the VUMC EHR (418,371 females and 333,653 males), by performing logistic regression analysis conditioned on gender, age and the self-reported ancestry as covariates in the regression model. For this analysis we used a total of 600,107 European, 103,209 African, 12,411 Asian and 36,297 other ancestry patients, of which 222 were uncurated XFS cases (coded as 1) and the rest controls. To determine other health consequences of high genetic risk to XFS, we performed a PheWAS analysis [30] ($n = 52,251$) on the polygenic risk score generated from the Aung et al's. [36] XFS global dataset against patients genotyped on Illumina Mega-array chip in BioVU with about 18k ICD-9 /ICD-10 codes, accounting for age, gender, and the first 5 principal components.

Abbreviations

XFS	Exfoliation syndrome
GWAS	Genome-wide association study
TWAS	Transcriptomic Wide Association Studies
LD	Linkage Disequilibrium
eQTL	expression quantitative trait locus
DNA	Deoxyribonucleic acid
RNA	Ribonucleic acid
mRNA	Messenger RNA
MEGA	Multi-Ethnic Global Array
GTE _x	The Genotype-Tissue Expression project
MultiXcan	Multi-Tissue PrediXcan
SUGEN	Genetic Association Analysis Under Complex Survey Sampling
GSEA	Gene Set Enrichment Analysis
EHR	Electronic Health Record
PheWAS	phenome-wide association analysis
PCR	Polymerase Chain Reactions
PUFA	polyunsaturated fatty acid
IOP	Intra-Ocular Pressure

Supplementary Information

The online version contains supplementary material available at <https://doi.org/10.1186/s12864-023-09179-7>.

Additional file 1.

Acknowledgements

We are grateful to Maria Niarchou and Tyne Fleming for comments on earlier version of the manuscript.

Authors' contributions

JH, NJC and ERG jointly conceived the project. AR, USS, DB and FP managed patients' data and tissues' samples of the three European cohorts. AR, USS, DB and FP conducted functional biological experiments. FP contributed raw genotyping data for European populations. JH performed all the statistical analysis. JS, RT, PSS, AIK, MAB1, PE & PP helped scripts and statistical analysis. JH, RT, KJ, NJC, ERG, MAB2, FP & CCK were involved in interpretation of data. JH drafted the manuscript with critical input from KJ, NJC, ERG, FP & CCK. The manuscript was also critiqued and approved by all authors. NJC was responsible for obtaining financial support for this study.

Funding

JH was jointly supported through grant to MAB2 (T32 grant 5T32EY021453), ERG and NJC. ERG is grateful to the President and Fellows of Clare Hall, University of Cambridge for the fellowship support. ERG is also supported by a NIH Genomic Innovator Award (R35HG010718). The content is solely the responsibility of the authors and does not necessarily represent the official views of the National Institutes of Health. KMJ – Joseph Ellis Family and William Black Research Funds, NEI Core Grant 6P30EY08126 to Vanderbilt Vision Research Center, Unrestricted Departmental Grant from Research to Prevent Blindness, Inc., NY. The European-Data-Set was support by the Interdisciplinary Center for Clinical Research (IZKF) at the University Hospital of the University of Erlangen-Nuremberg (project E23) to AR and USS and the Deutsche Forschungsgemeinschaft (SCHL 366/8–1) to USS. The funding bodies played no role in the design of the study and collection, analysis, and interpretation of data and in writing the manuscript.

Availability of data and materials

Multi-ethnic Summary data can be obtained from <https://www.nature.com/articles/ng.3875>
European subset summary data obtained from the link on this study.
Other Important Links for additional data and models:
<https://github.com/gamazonlab/MR-JTI> for links to predixcan models.
<https://ftp.1000genomes.ebi.ac.uk/vol1/ftp/phase3/>
<https://www.ebi.ac.uk/gwas/>
<https://gtexportal.org/home/>

Declarations

Ethics approval and consent to participate

Informed consent to tissue donation was obtained from the donors or from relatives for those who are deceased. The protocol of the study was approved by the Ethics Committee of the Medical Faculty of the Friedrich-Alexander-Universität Erlangen-Nürnberg (No. 4218-CH) and adhered to the tenets of the Declaration of Helsinki for experiments involving human tissues and samples.

Consent for publication

N/A.

Competing interests

ERG receives an honorarium from the journal *Circulation Research* of the American Heart Association, as a member of the Editorial Board. The remaining authors declare no competing interests.

Author details

¹Genetic Medicine, Vanderbilt University School of Medicine, Nashville, TN 37232, USA. ²Vanderbilt Genetics Institute, Nashville, TN 37232, USA. ³Institute of Human Genetics, Friedrich-Alexander-Universität Erlangen-Nürnberg FAU, 91054 Erlangen, Germany. ⁴Clare Hall and MRC Epidemiology Unit, University of Cambridge, Cambridge CB2 0SL, UK. ⁵Vanderbilt Eye Institute, Vanderbilt University Medical Center, Nashville, TN 37232, USA. ⁶Department of Ophthalmology, Universitätsklinikum Erlangen, Friedrich-Alexander-Universität Erlangen-Nürnberg, 91054 Erlangen, Germany. ⁷Biostatistics, Vanderbilt University School of Medicine, Nashville, TN 37232, USA. ⁸Genome Institute of Singapore, 60 Biopolis St, Singapore 138672, Singapore.

Received: 20 June 2022 Accepted: 9 February 2023
Published online: 16 February 2023

References

- Schlötzer-Schrehardt U. Genetics and genomics of pseudoexfoliation syndrome/glaucoma. *Middle East Afr J Ophthalmol*. 2011;18:30–6. <https://doi.org/10.4103/0974-9233.75882>.
- Schlötzer-Schrehardt U, Naumann GOH. Ocular and systemic Pseudoexfoliation syndrome. *Am J Ophthalmol*. 2006;141:921–937.e2. <https://doi.org/10.1016/j.ajo.2006.01.047>.
- Davis RE, Schuman JS. Pseudoexfoliation syndrome: don't brush it off. *Br J Ophthalmol*. 2013;97:1091–2. <https://doi.org/10.1136/bjophthalmol-2012-302417>.
- Mastronikolis S, Pagkalou M, Baroutas G, Kyriakopoulou K, Makri OE, Georgakopoulos CD. Pseudoexfoliation syndrome: the critical role of the extracellular matrix in pathogenesis and treatment. *IUBMB Life*. 2022;74:995–1002. <https://doi.org/10.1002/iub.2606>.
- Botling Taube A, Konzer A, Alm A, Bergquist J. Proteomic analysis of the aqueous humour in eyes with pseudoexfoliation syndrome. *Br J Ophthalmol*. 2019;103:1190–4. <https://doi.org/10.1136/bjophthalmol-2017-310416>.
- Rebecca M, Gayathri R, Bhuvanansundar R, Sriprya K, Shantha B, Angayarkanni N. Elastin modulation and modification by homocysteine: a key factor in the pathogenesis of Pseudoexfoliation syndrome? *Br J Ophthalmol*. 2018;103:985–92. <https://doi.org/10.1136/bjophthalmol-2018-312088>.
- Vesti E, Kivelä T. Exfoliation syndrome and exfoliation glaucoma. *Prog Retin Eye Res*. 2000;19:345–68. [https://doi.org/10.1016/S1350-9462\(99\)00019-1](https://doi.org/10.1016/S1350-9462(99)00019-1).
- Chung H, Arora S, Damji KF, Weis E. Association of pseudoexfoliation syndrome with cardiovascular and cerebrovascular disease: a systematic review and meta-analysis. *Can J Ophthalmol*. 2018;53:365–72. <https://doi.org/10.1016/j.cjco.2017.10.039>.
- Andrikopoulos GK, Alexopoulos DK, Gartaganis SP. Pseudoexfoliation syndrome and cardiovascular diseases. *World J Cardiol*. 2014;6:847–54. <https://doi.org/10.4330/wjcv.6.i8.847>.
- Pasutto F, Zenkel M, Hoja U, Berner D, Uebe S, Ferrazzi F, et al. Pseudoexfoliation syndrome-associated genetic variants affect transcription factor binding and alternative splicing of LOXL1. *Nat Commun*. 2017;8:15466.
- Xu F, Zhang L, Li M. Plasma homocysteine, serum folic acid, serum vitamin B12, serum vitamin B6, MTHFR and risk of pseudoexfoliation glaucoma: a meta-analysis. *Graefes Arch Clin Exp Ophthalmol*. 2012;250:1067–74. <https://doi.org/10.1007/s00417-011-1877-4>.
- Clement CI, Goldberg I, Healey PR, Graham SL. Plasma homocysteine, MTHFR gene mutation, and open-angle Glaucoma. *J Glaucoma*. 2009;18:73–8.
- Aasved H. Study of relatives of persons with fibrillogluthia epitheliocapsularis (Pseudoexfoliation of the lens capsule). *Acta Ophthalmol*. 1975;53:879–86. <https://doi.org/10.1111/j.1755-3768.1975.tb00406.x>.
- Gottfredsdottir MS, Sverrisson T, Musch DC, Stefansson E. Chronic open-angle Glaucoma and associated ophthalmic findings in monozygotic twins and their spouses in Iceland. *J Glaucoma*. 1999;8:134–9.
- Aung T, Ozaki M, Mizoguchi T, Allingham RR, Li Z, Haripriya A, et al. A common variant mapping to CACNA1A is associated with susceptibility to exfoliation syndrome. *Nat Genet*. 2015;47:387–92. <https://doi.org/10.1038/ng.3226>.
- Thorleifsson G, Magnusson KP, Sulem P, Walters GB, Gudbjartsson DF, Stefansson H, et al. Common sequence variants in the LOXL1 gene confer susceptibility to exfoliation Glaucoma. *Science*. 2007;317:1397–400. <https://doi.org/10.1126/science.1146554>.
- Krumbiegel M, Pasutto F, Schlötzer-Schrehardt U, Uebe S, Zenkel M, Mardin CY, et al. Genome-wide association study with DNA pooling identifies variants at CNTNAP2 associated with pseudoexfoliation syndrome. *Eur J Hum Genet EJHG*. 2011;19:186–93. <https://doi.org/10.1038/ejhg.2010.144>.
- Nakano M, Ikeda Y, Tokuda Y, Fuwa M, Ueno M, Imai K, et al. Novel common variants and susceptible haplotype for exfoliation glaucoma specific to Asian population. *Sci Rep*. 2014;4:5340.
- Zagajewska K, Piątkowska M, Goryca K, Bałabas A, Kluska A, Paziewska A, et al. GWAS links variants in neuronal development and actin remodeling related loci with pseudoexfoliation syndrome without glaucoma. *Exp Eye Res*. 2018;168:138–48. <https://doi.org/10.1016/j.exer.2017.12.006>.
- Craig JE, Hewitt AW, McMellon AE, Henders AK, Ma L, Wallace L, et al. Rapid inexpensive genome-wide association using pooled whole blood. *Genome Res*. 2009;19:2075–80. <https://doi.org/10.1101/gr.094680.109>.
- Aung T, Ozaki M, Lee MC, Schlötzer-Schrehardt U, Thorleifsson G, Mizoguchi T, et al. Genetic association study of exfoliation syndrome identifies a protective rare variant at LOXL1 and five new susceptibility loci. *Nat Genet*. 2017;49:993–1004. <https://doi.org/10.1038/ng.3875>.
- Thomassin L, Werneck CC, Broekelmann TJ, Gleyzal C, Hornstra IK, Mechem RP, et al. The pro-regions of Lysyl oxidase and Lysyl oxidase-like 1 are required for deposition onto elastic fibers*. *J Biol Chem*. 2005;280:42848–55. <https://doi.org/10.1074/jbc.M506832200>.
- Mori K, Imai K, Matsuda A, Ikeda Y, Naruse S, Hitora-Takeshita H, et al. LOXL1 genetic polymorphisms are associated with exfoliation glaucoma in the Japanese population. *Mol Vis*. 2008;14:1037–40.
- Chen L, Jia L, Wang N, Tang G, Zhang C, Fan S, et al. Evaluation of LOXL1 polymorphisms in exfoliation syndrome in a Chinese population. *Mol Vis*. 2009;15:2349–57.
- Williams SEI, Whigham BT, Liu Y, Carmichael TR, Qin X, Schmidt S, et al. Major LOXL1 risk allele is reversed in exfoliation glaucoma in a black south African population. *Mol Vis*. 2010;16:705–12.
- Ozaki M, Lee KYC, Vithana EN, Yong VH, Thalamuthu A, Mizoguchi T, et al. Association of LOXL1 gene polymorphisms with Pseudoexfoliation in the Japanese. *Invest Ophthalmol Vis Sci*. 2008;49:3976–80. <https://doi.org/10.1167/iovs.08-1805>.
- Sharma S, Martin S, Sykes MJ, Dave A, Hewitt AW, Burdon KP, et al. Biological effect of LOXL1 coding variants associated with pseudoexfoliation syndrome. *Exp Eye Res*. 2016;146:212–23. <https://doi.org/10.1016/j.exer.2016.03.013>.
- Kim S, Kim Y. Variations in LOXL1 associated with exfoliation glaucoma do not affect amine oxidase activity. *Mol Vis*. 2012;18:265–70.
- Berner D, Hoja U, Zenkel M, Ross JJ, Uebe S, Paoli D, et al. The protective variant rs7173049 at LOXL1 locus impacts on retinoic acid signaling pathway in pseudoexfoliation syndrome. *Hum Mol Genet*. 2019;28:2531–48. <https://doi.org/10.1093/hmg/ddz075>.
- Hauser MA, Aboobakar IF, Liu Y, Miura S, Whigham BT, Challa P, et al. Genetic variants and cellular stressors associated with exfoliation syndrome modulate promoter activity of a lncRNA within the LOXL1 locus. *Hum Mol Genet*. 2015;24:6552–63. <https://doi.org/10.1093/hmg/ddv347>.
- Gamazon ER, Wheeler HE, Shah KP, Mozaffari SV, Aquino-Michaels K, Carroll RJ, et al. A gene-based association method for mapping traits using reference transcriptome data. *Nat Genet*. 2015;47:1091–8.
- Barbeira AN, Pividori M, Zheng J, Wheeler HE, Nicolae DL, Im HK. Integrating predicted transcriptome from multiple tissues improves association detection. *PLoS Genet*. 2019;15:e1007889. <https://doi.org/10.1371/journal.pgen.1007889>.
- Aguet F, Anand S, Ardlie KG, Gabriel S, Getz GA, Graubert A, et al. The GTEx consortium atlas of genetic regulatory effects across human tissues. *Science*. 2020;369:1318–30. <https://doi.org/10.1126/science.aaz1776>.
- Aguet F, Brown AA, Castel SE, Davis JR, He Y, Jo B, et al. Genetic effects on gene expression across human tissues. *Nature*. 2017;550:204–13. <https://doi.org/10.1038/nature24277>.
- Wainberg M, Sinnott-Armstrong N, Mancuso N, Barbeira AN, Knowles DA, Golan D, et al. Opportunities and challenges for transcriptome-wide association studies. *Nat Genet*. 2019;51:592–9. <https://doi.org/10.1038/s41588-019-0385-z>.
- Huang DW, Sherman BT, Lempicki RA. Bioinformatics enrichment tools: paths toward the comprehensive functional analysis of large gene lists. *Nucleic Acids Res*. 2009;37:1–13. <https://doi.org/10.1093/nar/gkn923>.
- Wagner AH, Anand VN, Wang W-H, Chatterton JE, Sun D, Shepard AR, et al. Exon-level expression profiling of ocular tissues. *Exp Eye Res*. 2013;111:105–11. <https://doi.org/10.1016/j.exer.2013.03.004>.

38. Thul PJ, Åkesson L, Wiking M, Mahdessian D, Geladaki A, Ait Blal H, et al. A subcellular map of the human proteome. *Science*. 2017;356:eaal3321. <https://doi.org/10.1126/science.aal3321>.
39. Uhlén M, Fagerberg L, Hallström BM, Lindskog C, Oksvold P, Mardinnoglu A, et al. Tissue-based map of the human proteome. *Science*. 2015;347:1260419. <https://doi.org/10.1126/science.1260419>.
40. Chen EY, Tan CM, Kou Y, Duan Q, Wang Z, Meirelles GV, et al. Enrichr: interactive and collaborative HTML5 gene list enrichment analysis tool. *BMC Bioinformatics*. 2013;14:128. <https://doi.org/10.1186/1471-2105-14-128>.
41. Kuleshov MV, Jones MR, Rouillard AD, Fernandez NF, Duan Q, Wang Z, et al. Enrichr: a comprehensive gene set enrichment analysis web server 2016 update. *Nucleic Acids Res*. 2016;44:W90–7. <https://doi.org/10.1093/nar/gkw377>.
42. Cornelis MC, Monda KL, Yu K, Paynter N, Azzato EM, Bennett SN, et al. Genome-wide meta-analysis identifies regions on 7p21 (AHR) and 15q24 (CYP1A2) as determinants of habitual caffeine consumption. *PLoS Genet*. 2011;7:e1002033. <https://doi.org/10.1371/journal.pgen.1002033>.
43. Amin N, Byrne E, Johnson J, Chenevix-Trench G, Walter S, Nolte IM, et al. Genome-wide association analysis of coffee drinking suggests association with CYP1A1/CYP1A2 and NRCAM. *Mol Psychiatry*. 2012;17:1116–29. <https://doi.org/10.1038/mp.2011.101>.
44. Cornelis MC, Kacprowski T, Menni C, Gustafsson S, Pivin E, Adamski J, et al. Genome-wide association study of caffeine metabolites provides new insights to caffeine metabolism and dietary caffeine-consumption behavior. *Hum Mol Genet*. 2016;25:5472–82. <https://doi.org/10.1093/hmg/ddw334>.
45. Feitosa MF, Kraja AT, Chasman DI, Sung YJ, Winkler TW, Ntalla I, et al. Novel genetic associations for blood pressure identified via gene-alcohol interaction in up to 570K individuals across multiple ancestries. *PLoS One*. 2018;13:e0198166. <https://doi.org/10.1371/journal.pone.0198166>.
46. Coffee and Caffeine Genetics Consortium, Cornelis MC, Byrne EM, Esko T, Nalls MA, Ganna A, et al. Genome-wide meta-analysis identifies six novel loci associated with habitual coffee consumption. *Mol Psychiatry*. 2015;20:647–56. <https://doi.org/10.1038/mp.2014.107>.
47. Li Y, Yao J, Han C, Yang J, Chaudhry MT, Wang S, et al. Quercetin, inflammation and immunity. *Nutrients*. 2016;8:167. <https://doi.org/10.3390/nu8030167>.
48. Simmons DL, Wagner D, Westover K. Nonsteroidal anti-inflammatory drugs, acetaminophen, cyclooxygenase 2, and fever. *Clin Infect Dis*. 2000;31:S211–8. <https://doi.org/10.1086/317517>.
49. Kraan J, van den Broek P, Verhoef C, Grunhagen DJ, Taal W, Gratama JW, et al. Endothelial CD276 (B7-H3) expression is increased in human malignancies and distinguishes between normal and tumour-derived circulating endothelial cells. *Br J Cancer*. 2014;111:149–56.
50. Wood JJ, Boyne JR, Paulus C, Jackson BR, Nevels MM, Whitehouse A, et al. ARID3B: a novel regulator of the Kaposi's sarcoma-associated herpesvirus lytic cycle. *J Virol*. 2016;90:9543–55. <https://doi.org/10.1128/JVI.03262-15>.
51. Lin C, Song W, Bi X, Zhao J, Huang Z, Li Z, et al. Recent advances in the ARID family: focusing on roles in human cancer. *OncoTargets Ther*. 2014;7:315–24. <https://doi.org/10.2147/OTT.S57023>.
52. Jeong YJ, Park SH, Mun SH, Kwak SG, Lee S-J, Oh HK. Association between lysyl oxidase and fibrotic focus in relation with inflammation in breast cancer. *Oncol Lett*. 2018;15:2431–40. <https://doi.org/10.3892/ol.2017.7617>.
53. Burgoyne RD, Morgan A. Secretory granule exocytosis. *Physiol Rev*. 2003;83:581–632. <https://doi.org/10.1152/physrev.00031.2002>.
54. Liu L, Guo Z, Tieu Q, Castle A, Castle D. Role of secretory carrier membrane protein SCAMP2 in granule exocytosis. *Mol Biol Cell*. 2002;13:4266–78. <https://doi.org/10.1091/mbc.e02-03-0136>.
55. Blank U, Madera-Salcedo IK, Danelli L, Claver J, Tiwari N, Sánchez-Miranda E, et al. Vesicular trafficking and signaling for cytokine and chemokine secretion in mast cells. *Front Immunol*. 2014;5:453. <https://doi.org/10.3389/fimmu.2014.00453>.
56. Chen X, Li Y, Blankson S, Liu M, Huang D, Redmond HP, et al. B7-H3 augments inflammatory responses and exacerbates brain damage via amplifying NF- κ B p65 and MAPK p38 activation during experimental pneumococcal meningitis. *PLoS One*. 2017;12:e0171146. <https://doi.org/10.1371/journal.pone.0171146>.
57. Zhang G, Wang J, Kelly J, Gu G, Hou J, Zhou Y, et al. B7-H3 augments the inflammatory response and is associated with human Sepsis. *J Immunol*. 2010;185:3677–84. <https://doi.org/10.4049/jimmunol.0904020>.
58. Hu H, Sun S-C. Ubiquitin signaling in immune responses. *Cell Res*. 2016;26:457–83.
59. Wu Y, Kang J, Zhang L, Liang Z, Tang X, Yan Y, et al. Ubiquitination regulation of inflammatory responses through NF- κ B pathway. *Am J Transl Res*. 2018;10:881–91.
60. Corn JE, Vucic D. Ubiquitin in inflammation: the right linkage makes all the difference. *Nat Struct Amp Mol Biol*. 2014;21:297–300.
61. Shetty R, Ghosh A, Lim RR, Subramani M, Mihir K, Reshma AR, et al. Elevated expression of matrix Metalloproteinase-9 and inflammatory cytokines in Keratoconus patients is inhibited by cyclosporine A. *Invest Ophthalmol Vis Sci*. 2015;56:738–50. <https://doi.org/10.1167/iov.14-14831>.
62. Kohli P, Levy BD. Resolvins and protectins: mediating solutions to inflammation. *Br J Pharmacol*. 2009;158:960–71. <https://doi.org/10.1111/j.1476-5381.2009.00290.x>.
63. Stark DT, Bazan NG. Neuroprotectin D1 induces neuronal survival and downregulation of Amyloidogenic processing in Alzheimer's disease cellular models. *Mol Neurobiol*. 2011;43:131–8. <https://doi.org/10.1007/s12035-011-8174-4>.
64. Huang W-B, Fan Q, Zhang X-L. Cod liver oil: a potential protective supplement for human glaucoma. *Int J Ophthalmol*. 2011;4:648–51. <https://doi.org/10.3980/j.issn.2222-3959.2011.06.15>.
65. Nguyen CTO, Bui BV, Sinclair AJ, Vingrys AJ. Dietary omega 3 fatty acids decrease intraocular pressure with age by increasing aqueous outflow. *Invest Ophthalmol Vis Sci*. 2007;48:756–62. <https://doi.org/10.1167/iov.06-0585>.
66. Mildemberger J, Johansson I, Sergin I, Kjøbli E, Damås JK, Razani B, et al. N-3 PUFAs induce inflammatory tolerance by formation of KEAP1-containing SQSTM1/p62-bodies and activation of NFE2L2. *Autophagy*. 2017;13:1664–78. <https://doi.org/10.1080/15548627.2017.1345411>.
67. Dewundara SS, Wiggs JL, Sullivan DA, Pasquale LR. Is estrogen a therapeutic target for Glaucoma? *Semin Ophthalmol*. 2016;31:140–6. <https://doi.org/10.3109/08820538.2015.1114845>.
68. Kitaoka Y, Munemasa Y, Hayashi Y, Kuribayashi J, Koseki N, Kojima K, et al. Axonal protection by 17 β -estradiol through Thioredoxin-1 in tumor necrosis factor-induced optic neuropathy. *Endocrinology*. 2011;152:2775–85. <https://doi.org/10.1210/en.2011-0046>.
69. Caprioli J, Munemasa Y, Kwong JMK, Piri N. Overexpression of thioredoxins 1 and 2 increases retinal ganglion cell survival after pharmacologically induced oxidative stress, optic nerve transection, and in experimental glaucoma. *Trans Am Ophthalmol Soc*. 2009;107:161–5.
70. Yildirim Z, Yildirim F, Uçgun NI, Sepici-Dinçel A. The role of the cytokines in the pathogenesis of pseudoexfoliation syndrome. *Int J Ophthalmol*. 2013;6:50–3. <https://doi.org/10.3980/j.issn.2222-3959.2013.01.10>.
71. Zenkel M, Krysta A, Pasutto F, Juenemann A, Kruse FE, Schlötzer-Schrehardt U. Regulation of Lysyl oxidase-like 1 (LOXL1) and elastin-related genes by pathogenic factors associated with Pseudoexfoliation syndrome. *Invest Ophthalmol Vis Sci*. 2011;52:8488–95. <https://doi.org/10.1167/iov.11-8361>.
72. Türkylmaz K, Öner V, Kirbas A, Sevim MS, Sekeryapan B, Özgür G, et al. Serum YKL-40 levels as a novel marker of inflammation and endothelial dysfunction in patients with pseudoexfoliation syndrome. *Eye Lond Engl*. 2013;27:854–9. <https://doi.org/10.1038/eye.2013.92>.
73. Gonen T, Guzel S, Keskinborca KH. YKL-40 is a local marker for inflammation in patients with pseudoexfoliation syndrome. *Eye*. 2019;33:772–6. <https://doi.org/10.1038/s41433-018-0308-8>.
74. Sorkhabi R, Ghorbanihaghjo A, Ahoor M, Nahaei M, Rashtchizadeh N. High-sensitivity C-reactive protein and tumor necrosis factor alpha in Pseudoexfoliation syndrome. *Oman Med J*. 2013;28:16–9. <https://doi.org/10.5001/omj.2013.04>.
75. Yüksel N, Pirhan D, Altıntaş Ö, Çağlar Y. Systemic high-sensitivity C-reactive protein level in Pseudoexfoliation syndrome and Pseudoexfoliation Glaucoma. *J Glaucoma*. 2010;19:373–6.
76. Grubben MJ, Boers GH, Blom HJ, Broekhuizen R, de Jong R, van Rijt L, et al. Unfiltered coffee increases plasma homocysteine concentrations

- in healthy volunteers: a randomized trial. *Am J Clin Nutr.* 2000;71:480–4. <https://doi.org/10.1093/ajcn/71.2.480>.
77. Urgert R, van Vliet T, Zock PL, Katan MB. Heavy coffee consumption and plasma homocysteine: a randomized controlled trial in healthy volunteers. *Am J Clin Nutr.* 2000;72:1107–10. <https://doi.org/10.1093/ajcn/72.5.1107>.
 78. Bleich S, Roedel J, Von Ahsen N, Schlötzer-Schrehardt U, Reulbach U, Beck G, et al. Elevated homocysteine levels in aqueous humor of patients with pseudoexfoliation glaucoma. *Am J Ophthalmol.* 2004;138:162–4. <https://doi.org/10.1016/j.ajo.2004.02.027>.
 79. Muqaku B, Tahir A, Klepeisz P, Bileck A, Kreutz D, Mayer RL, et al. Coffee consumption modulates inflammatory processes in an individual fashion. *Mol Nutr Food Res.* 2016;60:2529–41. <https://doi.org/10.1002/mnfr.201600328>.
 80. Furman D, Chang J, Lartigou L, Bolen CR, Haddad F, Gaudilliere B, et al. Expression of specific inflammasome gene modules stratifies older individuals into two extreme clinical and immunological states. *Nat Med.* 2017;23:174–84.
 81. Rivera-Oliver M, Diaz-Ríos M. Using caffeine and other adenosine receptor antagonists and agonists as therapeutic tools against neurodegenerative diseases: a review. *Life Sci.* 2014;101:1–9. <https://doi.org/10.1016/j.lfs.2014.01.083>.
 82. Berner D, Zenkel M, Pasutto F, Hoja U, Liravi P, Gusek-Schneider GC, et al. Posttranscriptional regulation of LOXL1 expression via alternative splicing and nonsense-mediated mRNA decay as an adaptive stress response. *Invest Ophthalmol Vis Sci.* 2017;58:5930–40. <https://doi.org/10.1167/iovs.17-22963>.
 83. Bobbs A, Gellerman K, Hallas WM, Joseph S, Yang C, Kurkewich J, et al. ARID3B directly regulates ovarian Cancer promoting genes. *PLoS One.* 2015;10:e0131961. <https://doi.org/10.1371/journal.pone.0131961>.
 84. Ovodenko B, Rostagno A, Neubert TA, Shetty V, Thomas S, Yang A, et al. Proteomic analysis of exfoliation deposits. *Invest Ophthalmol Vis Sci.* 2007;48:1447–57. <https://doi.org/10.1167/iovs.06-0411>.
 85. Srinivasan K, Strickland P, Valdes A, Shin GC, Hinck L. Netrin-1/Neogenin interaction stabilizes multipotent progenitor cap cells during mammary gland morphogenesis. *Dev Cell.* 2003;4:371–82. [https://doi.org/10.1016/S1534-5807\(03\)00054-6](https://doi.org/10.1016/S1534-5807(03)00054-6).
 86. Surena V, Nazemi SB, Fahimeh R, Mahshid N. Effects of cyclosporine and phenytoin on biomarker expressions in gingival fibroblasts of children and adults: an in vitro study. *J Basic Clin Physiol Pharmacol.* 2013;25:167–73. <https://doi.org/10.1515/jbcpp-2013-0003>.
 87. Takahashi N, Hayano T, Suzuki M. Peptidyl-prolyl cis-trans isomerase is the cyclosporin A-binding protein cyclophilin. *Nature.* 1989;337:473–5. <https://doi.org/10.1038/337473a0>.
 88. Seet L-F, Toh LZ, Finger SN, Chu SWL, Stefanovic B, Wong TT. Valproic acid suppresses collagen by selective regulation of Smads in conjunctival fibrosis. *J Mol Med Berl Ger.* 2016;94:321–34. <https://doi.org/10.1007/s00109-015-1358-z>.
 89. Chu C, Deng J, Xiang L, Wu Y, Wei X, Qu Y, et al. Evaluation of epigallocatechin-3-gallate (EGCG) cross-linked collagen membranes and concerns on osteoblasts. *Mater Sci Eng C.* 2016;67:386–94. <https://doi.org/10.1016/j.msec.2016.05.021>.
 90. Carroll CC, Martineau K, Arthur KA, Huynh RT, Volper BD, Broderick TL. The effect of chronic treadmill exercise and acetaminophen on collagen and cross-linking in rat skeletal muscle and heart. *Am J Physiol-Regul Integr Comp Physiol.* 2014;308:R294–9. <https://doi.org/10.1152/ajpregu.00374.2014>.
 91. Yoon JS, Chae MK, Jang SY, Lee SY, Lee EJ. Antifibrotic effects of quercetin in primary orbital fibroblasts and orbital fat tissue cultures of graves' Orbitopathy. *Invest Ophthalmol Vis Sci.* 2012;53:5921–9. <https://doi.org/10.1167/iovs.12-9646>.
 92. Ganbold M, Shimamoto Y, Ferdousi F, Tominaga K, Isoda H. Antifibrotic effect of methylated quercetin derivatives on TGFβ-induced hepatic stellate cells. *Biochem Biophys Rep.* 2019;20:100678. <https://doi.org/10.1016/j.bbrep.2019.100678>.
 93. Donejko M, Przyłipiak A, Rysiak E, Gluszek K, Surażyński A. Influence of caffeine and hyaluronic acid on collagen biosynthesis in human skin fibroblasts. *Drug Des Devel Ther.* 2014;8:1923–8. <https://doi.org/10.2147/DDDT.S69791>.
 94. Gressner OA. About coffee, cappuccino and connective tissue growth factor—or how to protect your liver!? *Environ Toxicol Pharmacol.* 2009;28:1–10. <https://doi.org/10.1016/j.etap.2009.02.005>.
 95. Fehrholtz M, Glaser K, Speer CP, Seidenspinner S, Ottensmeier B, Kunzmann S. Caffeine modulates glucocorticoid-induced expression of CTGF in lung epithelial cells and fibroblasts. *Respir Res.* 2017;18:51. <https://doi.org/10.1186/s12931-017-0535-8>.
 96. Tatler AL, Barnes J, Habgood A, Goodwin A, McAnulty RJ, Jenkins G. Caffeine inhibits TGFβ activation in epithelial cells, interrupts fibroblast responses to TGFβ, and reduces established fibrosis in ex vivo precision-cut lung slices. *Thorax.* 2016;71:565–7. <https://doi.org/10.1136/thoraxjnl-2015-208215>.
 97. Cataldo A, Hamilton D, Barnett J, Paskevich P, Nixon R. Properties of the endosomal-lysosomal system in the human central nervous system: disturbances mark most neurons in populations at risk to degenerate in Alzheimer's disease. *J Neurosci.* 1996;16:186–99. <https://doi.org/10.1523/JNEUROSCI.16-01-00186.1996>.
 98. Taraboulos A, Raeber AJ, Borchelt DR, Serban D, Prusiner SB. Synthesis and trafficking of prion proteins in cultured cells. *Mol Biol Cell.* 1992;3:851–63. <https://doi.org/10.1091/mbc.3.8.851>.
 99. Kegel KB, Kim M, Sapp E, McIntyre C, Castañó JG, Aronin N, et al. Huntingtin Expression Stimulates Endosomal–Lysosomal Activity, Endosome Tubulation, and Autophagy. *J Neurosci.* 2000;20:7268–78. <https://doi.org/10.1523/JNEUROSCI.20-19-07268.2000>.
 100. Kumar P, Smith T, Raeman R, Chopky DM, Brink H, Liu Y, et al. Periostin promotes liver fibrogenesis by activating lysyl oxidase in hepatic stellate cells. *J Biol Chem.* 2018;293:12781–92. <https://doi.org/10.1074/jbc.RA117.001601>.
 101. Laczko R, Szauter KM, Csiszar K. LOXL1-associated candidate epithelial pathomechanisms in exfoliation glaucoma. *J Glaucoma.* 2014;23:543–7. <https://doi.org/10.1097/JG.000000000000105>.
 102. Zenkel M, Lewczuk P, Jünemann A, Kruse FE, Naumann GOH, Schlötzer-Schrehardt U. Proinflammatory cytokines are involved in the initiation of the abnormal matrix process in pseudoexfoliation syndrome/glaucoma. *Am J Pathol.* 2010;176:2868–79. <https://doi.org/10.2353/ajpath.2010.090914>.
 103. Wu B, Li Y, An C, Jiang D, Gong L, Liu Y, et al. High resolution profile of body wide pathological changes induced by abnormal elastin metabolism in Loxl1 knockout mice. *Cell Prolif.* 2021;54:e13077. <https://doi.org/10.1101/353169>.
 104. Donley D, Nelson R, Gigley J, Fox J. Mutant huntingtin protein alters the response of microglial cells to inflammatory stimuli. *bioRxiv.* 2019;550913. <https://doi.org/10.1101/550913>.
 105. Currais A, Quehenberger O, Armando M, A., Daugherty, D., Maher, P., and Schubert, D. Amyloid proteotoxicity initiates an inflammatory response blocked by cannabinoids. *Npj Aging Mech Dis.* 2016;2:16012.
 106. Ongen H, Brown AA, Delaneau O, Panousis NI, Nica AC, Dermitzakis ET, et al. Estimating the causal tissues for complex traits and diseases. *Nat Genet.* 2017;49:1676–83. <https://doi.org/10.1038/ng.3981>.
 107. Erkelens MN, Mebius RE. Retinoic acid and immune homeostasis: A balancing act. *Trends Immunol.* 2017;38:168–80. <https://doi.org/10.1016/j.it.2016.12.006>.
 108. Kim CH. In: Litwack G, editor. Chapter four - retinoic acid, immunity, and inflammation: Vitamins & Hormones, Academic Press; 2011. p. 83–101. <https://doi.org/10.1016/B978-0-12-386960-9.00004-6>.
 109. Pino-Lagos, K., Guo, Y., and Noelle, R.J. (2010). Retinoic acid: a key player in immunity. *BioFactors Oxf. Engl.* 36, 430–436. <https://doi.org/10.1002/biof.117>.
 110. Gamazon, E.R., Segrè, A.V., van de Bunt, M., Wen, X., Xi, H.S., Hormozdiari, F., Ongen, H., Konkashbaev, A., Derks, E.M., Aguet, F., et al. (2018). Using an atlas of gene regulation across 44 human tissues to inform complex disease- and trait-associated variation. *Nat. Genet.* 50, 956–967. <https://doi.org/10.1038/s41588-018-0154-4>.
 111. Machiela MJ, Chanock SJ. LDlink: a web-based application for exploring population-specific haplotype structure and linking correlated alleles of possible functional variants. *Bioinformatics.* 2015;31:3555–7. <https://doi.org/10.1093/bioinformatics/btv402>.
 112. Machiela MJ, Chanock SJ. LDassoc: an online tool for interactively exploring genome-wide association study results and prioritizing variants for functional investigation. *Bioinformatics.* 2017;34:887–9. <https://doi.org/10.1093/bioinformatics/btx561>.
 113. Lin D-Y, Tao R, Kalsbeek WD, Zeng D, Gonzalez F II, Fernández-Rhodes L, et al. Genetic Association Analysis under Complex Survey Sampling: The Hispanic Community Health Study/Study of Latinos. *Am. J. Hum. Genet.* 95:675–88. <https://doi.org/10.1016/j.ajhg.2014.11.005>.

114. Liao Y, Wang J, Jaehnig EJ, Shi Z, Zhang B. WebGestalt 2019: gene set analysis toolkit with revamped UIs and APIs. *Nucleic Acids Res.* 2019;47:W199–205. <https://doi.org/10.1093/nar/gkz401>.
115. Wang J, Vasaikar S, Shi Z, Greer M, Zhang B. WebGestalt 2017: a more comprehensive, powerful, flexible and interactive gene set enrichment analysis toolkit. *Nucleic Acids Res.* 2017;45:W130–7. <https://doi.org/10.1093/nar/gkx356>.
116. Wang J, Duncan D, Shi Z, Zhang B. WEB-based GENE SeT Analysis toolkit (WebGestalt): update 2013. *Nucleic Acids Res.* 2013;41:W77–83. <https://doi.org/10.1093/nar/gkt439>.
117. Zhang B, Kirov S, Snoddy J. WebGestalt: an integrated system for exploring gene sets in various biological contexts. *Nucleic acids res.* 2005;33:W741–8. <https://doi.org/10.1093/nar/gki475>.
118. Croft D, Mundo AF, Haw R, Milacic M, Weiser J, Wu G, et al. The Reactome pathway knowledgebase. *Nucleic Acids Res.* 2014;42:D472–7. <https://doi.org/10.1093/nar/gkt1102>.
119. Aguiar VRC, César J, Delaneau O, Dermitzakis ET, Meyer D. Expression estimation and eQTL mapping for HLA genes with a personalized pipeline. *PLoS Genet.* 2019;15:e1008091. <https://doi.org/10.1371/journal.pgen.1008091>.
120. Said I, Byrne A, Serrano V, Cardeno C, Vollmers C, Corbett-Detig R. Linked genetic variation and not genome structure causes widespread differential expression associated with chromosomal inversions. *Proc Natl Acad Sci.* 2018;115:5492–7. <https://doi.org/10.1073/pnas.1721275115>.
121. Denny JC, Ritchie MD, Basford MA, Pulley JM, Bastarache L, Brown-Gentry K, et al. PheWAS: demonstrating the feasibility of a phenome-wide scan to discover gene–disease associations. *Bioinformatics.* 2010;26:1205–10. <https://doi.org/10.1093/bioinformatics/btq126>.

Publisher's Note

Springer Nature remains neutral with regard to jurisdictional claims in published maps and institutional affiliations.

Ready to submit your research? Choose BMC and benefit from:

- fast, convenient online submission
- thorough peer review by experienced researchers in your field
- rapid publication on acceptance
- support for research data, including large and complex data types
- gold Open Access which fosters wider collaboration and increased citations
- maximum visibility for your research: over 100M website views per year

At BMC, research is always in progress.

Learn more biomedcentral.com/submissions

